

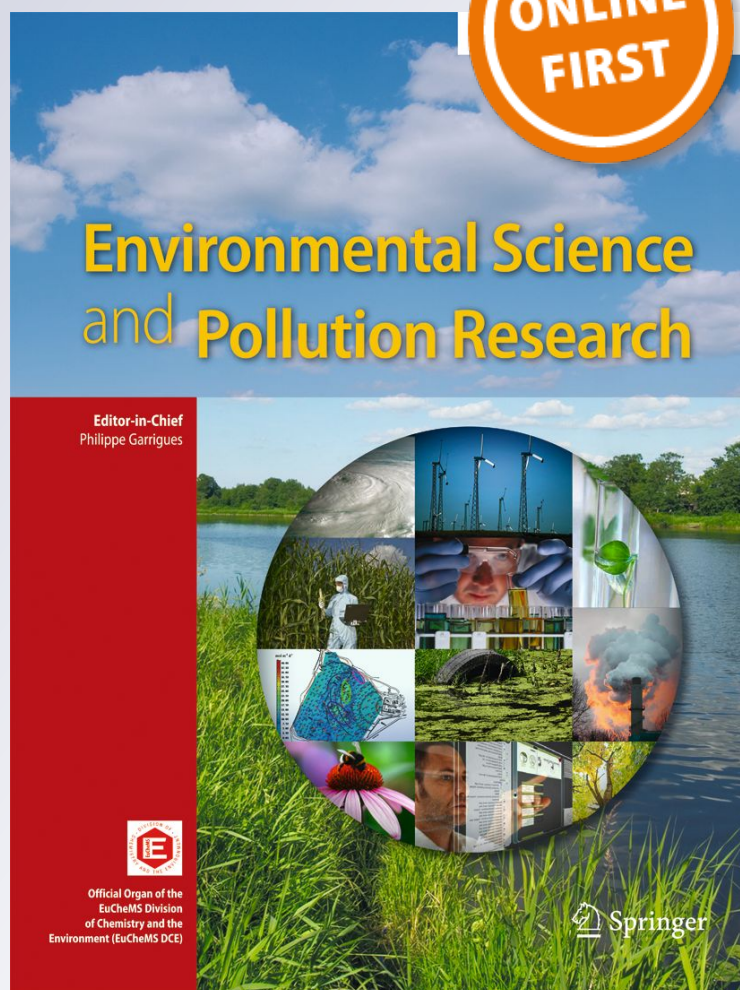
Absolute configuration of 2,2#,3,3#,6-pentachlorinatedbiphenyl (PCB 84) atropisomers

Xueshu Li, Sean R. Parkin & Hans-Joachim Lehmler

Environmental Science and Pollution Research


ISSN 0944-1344

Environ Sci Pollut Res
DOI 10.1007/s11356-017-9259-z



Your article is protected by copyright and all rights are held exclusively by Springer-Verlag Berlin Heidelberg. This e-offprint is for personal use only and shall not be self-archived in electronic repositories. If you wish to self-archive your article, please use the accepted manuscript version for posting on your own website. You may further deposit the accepted manuscript version in any repository, provided it is only made publicly available 12 months after official publication or later and provided acknowledgement is given to the original source of publication and a link is inserted to the published article on Springer's website. The link must be accompanied by the following text: "The final publication is available at link.springer.com".

Absolute configuration of 2,2',3,3',6-pentachlorinatedbiphenyl (PCB 84) atropisomers

Xueshu Li¹ · Sean R. Parkin² · Hans-Joachim Lehmler¹ Received: 16 December 2016 / Accepted: 10 May 2017
© Springer-Verlag Berlin Heidelberg 2017

Abstract Nineteen polychlorinated biphenyl (PCB) congeners, such as 2,2',3,3',6-pentachlorobiphenyl (PCB 84), display axial chirality because they form stable rotational isomers, or atropisomers, that are non-superimposable mirror images of each other. Although chiral PCBs undergo atropselective biotransformation and atropselectively alter biological processes, the absolute structure of only a few PCB atropisomers has been determined experimentally. To help close this knowledge gap, pure PCB 84 atropisomers were obtained by semi-preparative liquid chromatography with two serially connected Nucleodex β -PM columns. The absolute configuration of both atropisomers was determined by X-ray single-crystal diffraction. The PCB 84 atropisomer eluting first and second on the Nucleodex β -PM column correspond to (aR)-(-)-PCB 84 and (aS)-(+)-PCB 84, respectively. Enantioselective gas chromatographic analysis with the β -cyclodextrin-based CP-Chirasil-Dex CB gas chromatography column showed the same elution order as the Nucleodex β -PM column. Based on earlier reports, the atropisomers eluting first and second on the BGB-172 gas chromatography column are (aR)-(-)-PCB

84 and (aS)-(+)-PCB 84, respectively. An inversion of the elution order is observed on the Cyclosil-B gas chromatography and Cellulose-3 liquid chromatography columns. These results advance the interpretation of environmental and human biomonitoring as well as toxicological studies.

Keywords Absolute configuration · Chirality · Enantiomer · Environmental contaminant · Polychlorinated biphenyl · Rotational isomer

Introduction

Seventy-eight polychlorinated biphenyl (PCB) congeners out of the 209 possible congeners display axial chirality. However, only 19 of the 78 chiral congeners form rotational isomers, or atropisomers, that are stable at physiological temperature and under the conditions typically employed for enantioselective gas chromatographic analyses (Harju and Haglund 1999). These PCB congeners have a hindered rotation around the phenyl-phenyl bond due to the presence of three or four *ortho* chlorine substituents, with Gibbs-free energies of activation ($\Delta^\ddagger G$) of 176.6 to 184.8 kJ/mol for tri-*ortho* and ~246 kJ/mol for tetra-*ortho* substituted PCB congeners (Harju and Haglund 1999). Depending on the degree of chlorination, technical PCB mixtures contain between 0.15 and 33% by weight of chiral PCBs as racemic (i.e., 1:1) mixtures (Kania-Korwel and Lehmler 2016a). Based on published global production data, chiral PCBs make a significant contribution to the global environmental contamination with PCBs (Kania-Korwel and Lehmler 2016a), and some congeners, such as chiral PCB 95, are major congeners present in outdoor air (Grimm et al. 2015).

Responsible editor: Philippe Garrigues

Electronic supplementary material The online version of this article (doi:10.1007/s11356-017-9259-z) contains supplementary material, which is available to authorized users.

✉ Hans-Joachim Lehmler
hans-joachim-lehmler@uiowa.edu

¹ Department of Occupational and Environmental Health, College of Public Health, The University of Iowa, Iowa City, IA 52242, USA

² Department of Chemistry, University of Kentucky, Lexington, KY 40506, USA

The atropisomers of chiral PCB congeners differ in their environmental transport and fate due to atropselective biotransformation and other biological processes (Kania-Korwel and Lehmler 2016b; Lehmler et al. 2010). Following exposure to a racemic PCB mixture, chiral PCBs undergo considerable atropisomeric enrichment due to atropselective oxidation by cytochrome P450 enzymes in mammalian systems, including humans. For example, considerable enrichment of (+)-PCB 84 has been reported in mice following exposure to racemic PCB 84 (Lehmler et al. 2003). As with other chiral small molecules, PCB atropisomers differ in their biological activity and toxicity. Early toxicological studies demonstrate atropselective effects of pure PCB atropisomers on the induction of drug metabolizing enzymes (Püttmann et al. 1990, 1989; Rodman et al. 1991). Chiral PCBs atropselectively alter the gene expression of drug metabolizing enzymes and metabolism of amino acids in zebrafish (*Danio rerio*) embryos and larvae (Chai et al. 2016a, b; Xu et al. 2016). Moreover, several chiral PCB congeners, including PCB 84 and 2,2',3,3',6,6'-hexachlorobiphenyl (PCB 136), have been implicated in PCBs' developmental neurotoxicity, possibly by mechanisms involving altered cellular calcium homeostasis (Lehmler et al. 2005a; Pessah et al. 2009; Yang et al. 2014).

Pure atropisomers of chiral PCBs have been separated by enantioselective liquid chromatography (Haglund 1996a, b; Mannschreck et al. 1985; Toda et al. 2012; Xu et al. 2015; Yin et al. 2012) or were prepared in multistep syntheses (Püttmann et al. 1989, 1986), which allowed the determination of their optical rotation. Individual PCB atropisomers and their chiral metabolites are currently identified based on their optical rotation (Haglund 1996b) and their elution order on enantioselective gas chromatography or liquid chromatography columns (Haglund 1996b; Kania-Korwel and Lehmler 2013). However, it remains mostly unknown how the optical rotation and elution order of PCB atropisomers relate to their absolute structure. The absolute configurations of only a few PCB congeners and their metabolites have been reported to date. The absolute configuration of 2,2',3,3',4,4',5',6'-heptachlorobiphenyl (PCB 183) atropisomers was indirectly determined by comparing the experimental and theoretical circular dichroism spectra of pure atropisomers, with the atropisomers eluting first and second on the enantioselective HPLC column having the *aS* and *aR* configuration, respectively (Toda et al. 2012). A similar approach was used to determine the absolute structure of the atropisomers of several methoxy, methylthionyl, and methylsulfonyl metabolites of chiral PCBs (Pham-Tuan et al. 2005).

Determination of the absolute configuration using circular dichroism spectra of pure atropisomers is cumbersome because this approach requires the availability of relatively large (50 to 100 mg) quantities of pure PCB atropisomers and requires a comparison of experimental with theoretical circular dichroism spectra (Pham-Tuan et al. 2005; Toda et al. 2012).

Here we report the direct determination of the absolute structure of both PCB 84 atropisomers using X-ray crystal diffraction and, building on the absolute structure determination, establish the elution order of the (*aR*)- and (*aS*)-PCB 84 atropisomers on different enantioselective chromatography columns.

Materials and methods

Chemicals and reagents

HPLC-grade methanol (MeOH), tris(dibenzylideneacetone) dipalladium(0), and 2-dicyclohexylphosphino-2',6'-dimethoxybiphenyl were purchased from Sigma-Aldrich (Milwaukee, WI, USA). 2,3-Dichlorobenzeneboronic acid was obtained from Combi-blocks (San Diego, CA, USA). 2,3,6-Trichloriodobenzene was provided by Oakwood Products, Inc. (Estill, SC, USA). All solvents used for synthesis were purchased from Thermo Fisher Scientific (Waltham, MA, USA). Pesticide grade hexane was obtained from Fisher Scientific (Pittsburg, PA, USA). De-ionized, ultra-filtered water for the HPLC separations was obtained using a Milli-Q Academic A10 system (Millipore, Billerica, MA, USA).

Synthesis of racemic PCB 84

Racemic PCB 84 was synthesized from 2,3,6-trichloriodobenzene and 2,3-dichlorobenzeneboronic acid, with tris(dibenzylideneacetone)dipalladium(0)/2-dicyclohexylphosphino-2',6'-dimethoxybiphenyl as catalyst and potassium phosphate as base, using a modified Suzuki-coupling reaction as reported previously (Joshi et al. 2011). A colorless crystalline solid with a yield of 78% was obtained after purification of the crude reaction mixture with column chromatography on silica gel using hexane as eluent, followed by recrystallization in methanol. The racemic PCB 84 had a purity >99% based on relative peak area as determined by GC-MS.

HPLC separation and crystallization of PCB 84 atropisomers

Semi-preparative separation of PCB 84 atropisomers was performed on a Shimadzu high-performance liquid chromatography system consisting of a DGU-14A degasser, LC-10ATvp liquid chromatograph, SIL-10ADvp auto injector, SCL-10Avp system controller, CTO-20AC column oven, SPD-10Avp UV-VIS detector, and FRC-10A fraction collector (Shimadzu; Columbia, MD, USA) using two serially connected enantioselective Nucleodex β -PM columns (silica-based permethylated β -cyclodextrin, 4 mm \times 200 mm, 5 μ m; Macherey-Nagel, Duren, Germany) with MeOH/H₂O

(85:15, v/v) as mobile phase and a flow rate of 0.23 mL/min at 12 °C (Haglund 1996b; Lehmler et al. 2005a). The instrument was operated with LabSolutions software version 5.73 (Shimadzu). The general separation procedure was as follows: 20 µL of a saturated solution of racemic PCB 84 in HPLC grade methanol (approximately 5 mg/mL) was repeatedly injected into the HPLC system and fractions of both PCB 84 atropisomers were collected. Corresponding fractions were pooled and the mobile phase was evaporated under a gentle stream of nitrogen.

The residue was redissolved in 1 mL of hexane, the PCB 84 atropisomers were eluted with hexane through a glass pipette packed with 2 g of silica gel, and the solvent was removed under a gentle stream of nitrogen to give 38 mg of the first eluting atropisomer (i.e., (aR)-(-)-PCB 84) and 74 mg of the second eluting atropisomer (i.e., (aS)-(+)-PCB 84) starting from approximately 200 mg of racemic PCB 84. The overall purity of (aR)-(-)-PCB 84 and (aS)-(+)-PCB 84 were >99.9 and 99.3%, respectively, based on relative peak area.

Table 1 Crystal data and structure refinement for (aR)-PCB 84 [i.e., (-)-PCB 84], (aS)-PCB 84 [i.e., (+)-PCB 84] and (±)-PCB 84

Parameter	(aR)-(-)-PCB 84	(aS)-(+)-PCB 84	(±)-PCB 84 ^a
Empirical formula	C ₁₂ H ₅ Cl ₅		
Formula weight	326.41		
Temperature (K)	90.0(2)		173.0 (10)
Wavelength (Å)	1.54178		0.71073
Crystal system, space group	Orthorhombic, P2 ₁ 2 ₁ 2 ₁	Orthorhombic, P2 ₁ 2 ₁ 2 ₁	Monoclinic, P2 ₁ /c
<i>a</i> (Å)	<i>a</i> = 7.6560 (2)	7.6565 (2)	7.7015 (3)
<i>b</i> (Å)	<i>b</i> = 7.8060 (3)	7.8082 (2)	7.8357 (3)
<i>c</i> (Å)	<i>c</i> = 41.5633 (13)	41.5654 (11)	21.1617 (7)
<i>a</i> (°)	90	90	90
<i>β</i> (°)	90	90	99.9257 (17)
<i>γ</i> (°)	90	90	90
<i>V</i> (Å ³)	2483.94 (14)	2484.92 (11)	1257.92 (8)
<i>Z</i>	8	8	4
Calculated density (Mg m ⁻³)	1.746	1.746	1.724
Absorption coefficient (mm ⁻¹)	10.397	10.393	1.123
<i>F</i> (000)	1296	1296	648
Crystal size (mm)	0.20 × 0.12 × 0.03	0.28 × 0.24 × 0.14	0.28 × 0.20 × 0.06
<i>θ</i> range (°)	2.126–68.440	4.254–68.408	1.95–27.44
	–3 < <i>h</i> < 9	–9 < <i>h</i> < 9	–9 < <i>h</i> < 9
Limiting indices	–9 < <i>k</i> < 9	–9 < <i>k</i> < 9	–10 < <i>k</i> < 10
	–49 < <i>l</i> < 49	–20 < <i>l</i> < 49	–27 < <i>l</i> < 27
Reflections collected/unique	24,731/4352	27,324/4396	10,705/2861
<i>R</i> (int)	0.064	0.056	0.041
Completeness to <i>θ</i> = 27.44	97.3%	98.5%	98.5%
Max. and min. Transmission	0.753 and 0.349	0.273 and 0.144	0.936 and 0.744
Data/restraints/parameters	4352/0/307	4396/0/307	2861/0/154
Goodness-of-fit on <i>F</i> ²	1.08	1.19	1.04
Final <i>R</i> indices <i>I</i> > 2σ(<i>I</i>)	<i>R</i> ₁ = 0.041, <i>wR</i> ₁ = 0.100	<i>R</i> ₁ = 0.050, <i>wR</i> ₁ = 0.125	<i>R</i> ₁ = 0.032, <i>wR</i> ₁ = 0.073
<i>R</i> indices (all dat)	<i>R</i> ₁ = 0.043, <i>wR</i> ₁ = 0.110	<i>R</i> ₁ = 0.051, <i>wR</i> ₁ = 0.126	<i>R</i> ₁ = 0.045, <i>wR</i> ₁ = 0.078
Absolute structure parameter (<i>x</i>)	0.075 (9)	0.093 (9)	n/a
Largest diff. peak and hole (eÅ ⁻³)	0.50, –0.58	0.77, –0.48	0.34, –0.28

Computer programs: APEX2 (Bruker-AXS 2006), SADABS (Krause et al. 2015), XABS2 (Parkin et al. 1995), and the SHELX suite (Sheldrick 2008, 2015). For Flack *x* parameter, see Parsons et al. (2013)

^a The structure of (±)-PCB84 has been reported previously (Lehmler et al. 2005b)

Enantioselective gas chromatographic determinations

Racemic PCB 84 and pure PCB 84 atropisomers were analyzed on an Agilent 5975 GC system equipped with a ^{63}Ni -micro electron capture detector (μECD) and an Agilent CP-Chirasil-Dex CB capillary column with cyclodextrin directly bonded to dimethylpolysiloxane (25 m length, 0.25 mm inner diameter, 0.25 μm film thickness; Varian, Palo Alto, CA, USA). The temperature program for the enantioselective analysis was modified based on a published method (Kania-Korwel et al. 2006): starting temperature 50 $^{\circ}\text{C}$, hold for 1 min, 10 $^{\circ}\text{C}/\text{min}$ to 140 $^{\circ}\text{C}$, hold at 140 $^{\circ}\text{C}$ for 190 min, 10 $^{\circ}\text{C}/\text{min}$ to 225 $^{\circ}\text{C}$, and hold at 225 $^{\circ}\text{C}$ for 10 min. A constant flow rate of 3.0 mL/min was used. The injector was operated in the splitless mode at 250 $^{\circ}\text{C}$, and the detector temperature was 300 $^{\circ}\text{C}$. The resolution of the two atropisomers of racemic PCB 84 was 0.77 on the GC column, based on the equation, $R_s = (t_2 - t_1) / [0.5 \times (BW_1 + BW_2)]$, where t_1 , t_2 , BW_1 , and BW_2 are the retention time and baseline width of first and second eluting peaks.

The enantiomer fractions (EFs) of the PCB 84 atropisomer eluting first (i.e., (aR)-(-)-PCB 84) and second (i.e., (aS)-(+)-PCB 84) on the Nucleodex β -PM column were 0.02 and 0.98,

respectively. The percent enantiomer excess (ee) values of (aR)-(-)-PCB 84 and (aS)-(+)-PCB 84 were 97% ee and 96% ee, respectively. EF and ee values were calculated based on the equations $\text{EF} = A_{(+)} / [A_{(+)} + A_{(-)}]$ and $\text{ee}\% = |A_{(-)} - A_{(+)}| / [A_{(-)} + A_{(+)}] \times 100\%$, where $A_{(-)}$ and $A_{(+)}$ are the peak area of (aR)-(-)-PCB 84 and (aS)-(+)-PCB 84, respectively.

X-ray crystal structure analysis

Crystals of both PCB 84 atropisomers suitable for crystal structure analysis were obtained by slow evaporation of a solution of the respective atropisomer in methanol. X-ray diffraction data were collected at 90 K on a Bruker-Nonius X8 Proteum diffractometer in the X-ray Crystallography Facility in the Department of Chemistry at the University of Kentucky (Lexington, KY, USA) as described previously (Li et al. 2014). The crystal data and other relevant parameters are summarized in Table 1. A comparison of bond lengths and angles is provided in Tables 2 and 3. The molecular structure with the atom numbering scheme is shown in Fig. 1. Crystallographic data for the structures reported in this paper have been deposited with the Cambridge Crystallographic Data Centre, CCDC depositions 1522987 and 1522988. Copies of the data can be obtained, free of charge, on application to CCDC, 12 Union

Table 2 Comparison of bond lengths (\AA) of racemic PCB 84 and its two atropisomers

Bond lengths (\AA)	(aR)-(-)-PCB84		(aS)-(+)-PCB84		(\pm)-PCB84 ^a
	Molecule A ^b	Molecule B ^b	Molecule A ^b	Molecule B ^b	
C(1)-C(2)	1.395 (8)	1.396 (7)	1.406 (13)	1.399 (12)	1.390 (3)
C(1)-C(6)	1.396 (7)	1.397 (8)	1.409 (11)	1.408 (12)	1.399 (3)
C(1)-C(1')	1.494 (8)	1.493 (7)	1.490 (12)	1.474 (12)	1.491 (2)
C(2)-C(3)	1.387 (9)	1.394 (8)	1.377 (13)	1.382 (13)	1.392 (3)
C(2)-Cl(1)	1.724 (5)	1.723 (5)	1.724 (9)	1.730 (8)	1.7289 (19)
C(3)-C(4)	1.370 (7)	1.385 (7)	1.378 (12)	1.383 (11)	1.382 (3)
C(3)-Cl(2)	1.741 (6)	1.735 (6)	1.741 (10)	1.737 (9)	1.732 (2)
C(4)-C(5)	1.385 (9)	1.393 (8)	1.382 (13)	1.416 (13)	1.380 (3)
C(5)-C(6)	1.376 (8)	1.383 (8)	1.375 (13)	1.352 (13)	1.387 (3)
C(6)-Cl(3)	1.735 (6)	1.730 (5)	1.747 (9)	1.742 (9)	1.736 (2)
C(1')-C(2')	1.385 (8)	1.383 (8)	1.383 (13)	1.403 (12)	1.392 (3)
C(1')-C(6')	1.403 (8)	1.396 (8)	1.399 (13)	1.404 (12)	1.393 (3)
C(2')-C(3')	1.382 (8)	1.406 (8)	1.375 (14)	1.377 (12)	1.395 (3)
C(2')-Cl(4)	1.727 (6)	1.733 (5)	1.737 (9)	1.739 (9)	1.7288 (19)
C(3')-C(4')	1.392 (9)	1.367 (9)	1.405 (14)	1.364 (13)	1.384 (3)
C(3')-Cl(5)	1.730 (6)	1.740 (7)	1.725 (10)	1.732 (9)	1.728 (2)
C(4')-C(5')	1.389 (8)	1.392 (9)	1.413 (13)	1.410 (13)	1.382 (3)
C(5')-C(6')	1.402 (9)	1.377 (8)	1.392 (13)	1.381 (12)	1.383 (3)

^a The structure of (\pm)-PCB84 has been reported previously (Lehmler et al. 2005b)

^b There are two molecules (i.e., A and B) in the asymmetric unit of the crystal of each atropisomer

Table 3 Comparison of bond angles ($^{\circ}$) of racemic PCB 84 and its two atropisomers

Bond angle ($^{\circ}$)	(aR)-(-)-PCB84		(aS)-(+)-PCB84		(\pm) -PCB84 ^a
	Molecule A ^b	Molecule B ^b	Molecule A ^b	Molecule B ^b	
C(2)-C(1)-C(6)	117.6 (5)	118.0 (5)	116.2 (8)	116.5 (8)	117.42 (17)
C(2)-C(1)-C(1')	121.3 (5)	121.0 (5)	122.3 (7)	122.3 (8)	121.35 (17)
C(6)-C(1)-C(1')	121.1 (5)	121.0 (5)	121.5 (8)	121.3 (7)	121.21 (17)
C(3)-C(2)-C(1)	120.4 (5)	120.2 (5)	120.9 (8)	120.8 (7)	120.69 (17)
C(3)-C(2)-Cl(1)	120.6 (5)	120.1 (4)	121.1 (7)	120.8 (6)	119.91 (15)
C(1)-C(2)-Cl(1)	119.0 (4)	119.7 (4)	118.0 (7)	118.4 (7)	119.40 (14)
C(4)-C(3)-C(2)	120.7 (6)	120.8 (5)	120.9 (9)	121.2 (8)	120.28 (18)
C(4)-C(3)-Cl(2)	119.0 (5)	118.7 (5)	120.1 (7)	120.2 (6)	119.09 (15)
C(2)-C(3)-Cl(2)	120.2 (4)	120.5 (4)	119.0 (7)	118.5 (7)	120.62 (15)
C(3)-C(4)-C(5)	119.9 (5)	119.6 (5)	120.3 (8)	118.6 (8)	120.12 (18)
C(6)-C(5)-C(4)	119.4 (5)	119.2 (5)	118.7 (8)	119.3 (8)	119.17 (18)
C(5)-C(6)-C(1)	122.0 (5)	122.1 (5)	123.1 (9)	123.6 (8)	122.32 (18)
C(5)-C(6)-Cl(3)	118.8 (4)	118.7 (4)	118.5 (7)	118.3 (6)	118.38 (15)
C(1)-C(6)-Cl(3)	119.2 (4)	119.2 (4)	118.4 (7)	118.1 (7)	119.30 (14)
C(6')-C(1')-C(2')	119.2 (5)	119.2 (5)	119.0 (8)	117.2 (8)	119.06 (17)
C(6')-C(1')-C(1)	119.6 (5)	121.4 (5)	122.0 (8)	123.5 (8)	119.61 (17)
C(2')-C(1')-C(1)	121.2 (5)	119.4 (5)	119.0 (8)	119.3 (8)	121.33 (16)
C(3')-C(2')-C(1')	120.0 (6)	119.8 (5)	121.5 (9)	121.3 (8)	120.07 (17)
C(3')-C(2')-Cl(4)	120.1 (4)	120.0 (4)	119.7 (8)	121.3 (7)	119.62 (14)
C(1')-C(2')-Cl(4)	119.9 (4)	120.2 (5)	118.8 (7)	117.3 (7)	120.31 (15)
C(2')-C(3')-C(4')	121.0 (5)	120.2 (6)	120.8 (9)	120.8 (8)	119.97 (19)
C(2')-C(3')-Cl(5)	120.8 (5)	119.7 (5)	121.4 (8)	119.2 (7)	120.62 (15)
C(4')-C(3')-Cl(5)	118.2 (5)	120.1 (5)	117.9 (7)	120.0 (7)	119.40 (15)
C(5')-C(4')-C(3')	119.1 (6)	120.3 (5)	117.9 (9)	119.8 (8)	120.18 (18)
C(4')-C(5')-C(6')	120.1 (6)	119.7 (5)	120.6 (9)	119.2 (8)	119.94 (19)
C(1')-C(6')-C(5')	120.5 (5)	120.8 (6)	120.3 (8)	121.6 (8)	120.78 (19)

^a The structure of (\pm) -PCB84 has been reported previously (Lehmler et al. 2005b)

^b There are two molecules (i.e., A and B) in the asymmetric unit of the crystal of each atropisomer

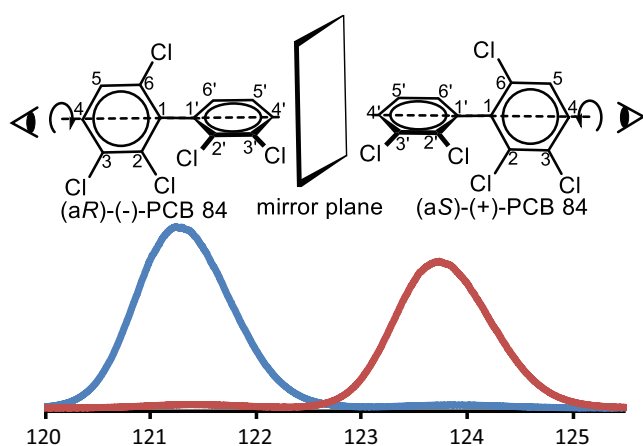


Fig. 1 (aR)-(-)-PCB 84 (blue line) elutes first and (aS)-(+)-PCB 84 (red line) elutes second on the enantioselective CP-Chirasil-Dex CB capillary column. The chemical structures of the PCB 84 atropisomers are shown above the corresponding peak in the gas chromatogram. Please see under “Materials and methods” for additional information regarding the enantioselective GC- μ ECD analysis

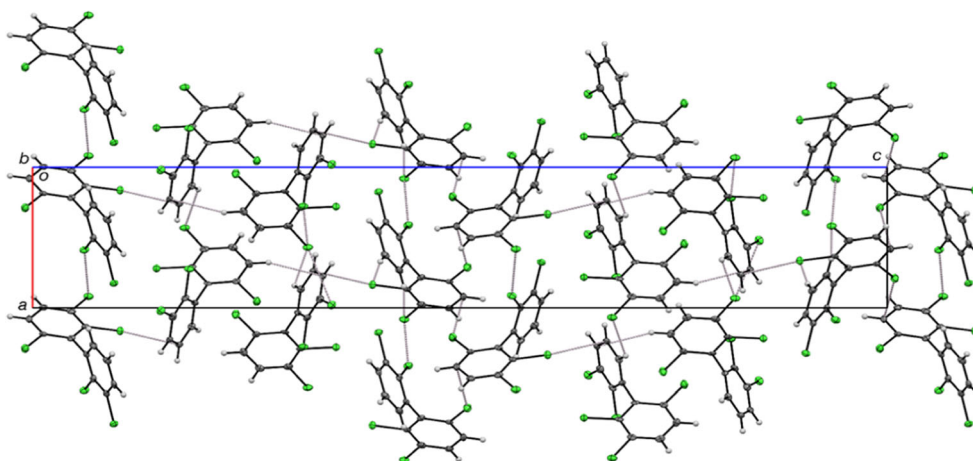
Road, Cambridge CB2 1EZ, UK, (fax: +44-(0)1223-336033 or e-mail: deposit@ccde.cam.ac.uk).

Results and discussion

Solid state structures

Both PCB 84 atropisomers crystallized in the orthorhombic space group $P2_12_12_1$, each with two molecules in the asymmetric unit, and packing together via van der Waals interactions. In the structure of (aR)-PCB84, the closest Cl \cdots Cl distances are 3.421(2) Å for Cl_{2a} \cdots Cl_{4a}(1 + x, y, z), 3.448 (2) Å for Cl_{2b} \cdots Cl_{4b}(1 + x, y - 1, z), and 3.4881(19) Å for Cl_{2b} \cdots Cl_{5b}(1 + x, y - 1, z), which are shorter than the van der Waals contact distances (Fig. 2). Not surprisingly, given the fact that the two structures are related by inversion, essentially, the same interactions are observed with (aS)-PCB84. The X-ray crystallographic analysis showed that the PCB 84

Fig. 2 View of van der Waals interaction between layers and intermolecular interactions by looking down the *b* axis of (*aR*)-(-)-PCB 84 X-ray diffraction. Cl⋯Cl, Cl⋯H, Cl⋯C, and C⋯H contacts are indicated with gray dotted lines



atropisomer eluting first and second on the chiral HPLC column (i.e., (-)-PCB 84 and (+)-PCB 84, respectively) have the *aR* and *aS* configuration, respectively. The two molecules in the asymmetric unit of (*aR*)-PCB84 (i.e., the atropisomer eluting first on the enantioselective HPLC column) displayed dihedral angles of $79.61(17)^\circ$ and $82.75(17)^\circ$ (Fig. 3). The dihedral angles of (*aS*)-PCB84 (i.e., the atropisomer eluting second on the enantioselective HPLC column) are very similar, at $79.6(3)^\circ$ and $82.8(3)^\circ$. These dihedral angles are close to the dihedral angle of $81.5(2)^\circ$ reported previously for racemic

PCB 84 (Lehmler et al. 2005b). In comparison, the experimental dihedral angles for non-, mono-, di-, tri-, and tetra-*ortho*-chlorine substituted PCB or PCB derivatives range from 5° to 42° for non-*ortho*-chlorine, 47° – 60° for mono-*ortho*-chlorine, 58° – 75° for di-*ortho*-chlorine, 69° – 87° for tri-*ortho*-chlorine, and 81° – 87° for tetra-*ortho*-chlorine containing PCBs, respectively (Table S1). This comparison demonstrates that the dihedral angle and, as a consequence, the three-dimensional structure of individual PCB congeners depend to a significant extent on the number of *ortho* chlorine

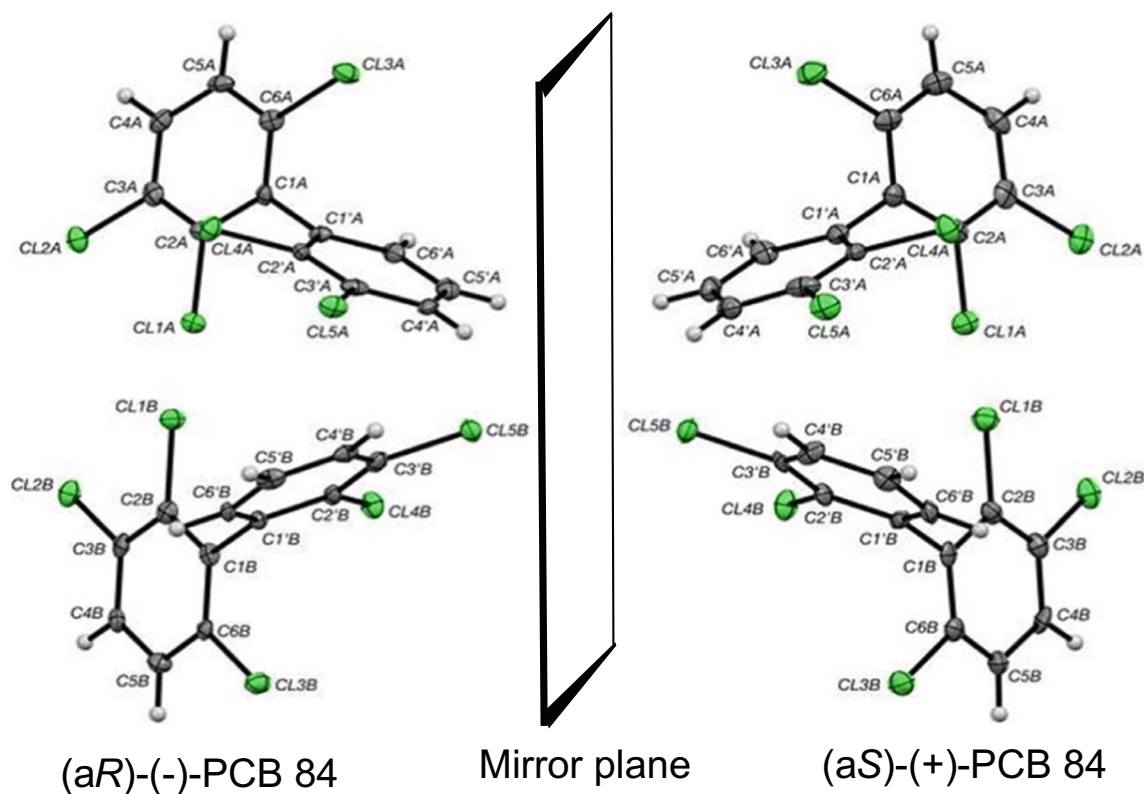


Fig. 3 Comparison of the asymmetric unit of (*aR*)-(-)-PCB 84 and (*aS*)-(+)-PCB 84. Displacement ellipsoids are drawn at the 50% probability level

Table 4 Elution order of PCB 84 atropisomers on different enantioselective liquid chromatography columns

Columns ^a	Mobile phase	Elution order		Reference
		Optical rotation (E_1/E_2)	Absolute structure (E_1/E_2)	
Nucleodex β -PM	MeOH-water	(-)/(+)	(aR)/(aS)	Haglund (1996b), Lehmler et al. (2005a), Reich and Schurig (1999); this work
Cellulose-3	<i>n</i> -Hexane	(+)(-)	(aS)/(aR)	Xu et al. (2015)
Cellulose-1	<i>n</i> -Hexane	NA		Yin et al. (2012)
Amylose-2	<i>n</i> -Hexane	NA		Yin et al. (2012)
Chiral-Dex	MeOH-TEAA	NA		Reich and Schurig (1999)
Chirasil-Dex modified silica gel	MeOH-TEAA	NA		Reich and Schurig (1999)

E_1 atropisomer eluting first on the column, E_2 atropisomer eluting second on the column, NA separable, but not assigned, TEAA triethylammonium acetate

^aThe Nucleodex β -PM column was from Macherey-Nagel (Düren, Germany); the Cellulose-1, Cellulose-3, and Amylose-2 columns were from Phenomenex (Guangzhou, China); and the Chiral-Dex column was from Merck (Kenilworth, NJ, USA)

substituents. Although chiral PCB congeners with three and four *ortho* chlorine substituents form stable rotational isomers under physiological conditions, congeners with only three *ortho* substituents have slightly smaller dihedral angles and are conformationally more flexible in the solid state than congeners with four *ortho* substituents. Further systematic studies are needed to assess how these slight structural differences influence the ability of chiral PCBs to interact with biological target molecules.

Elution order and absolute configuration of PCB 84 atropisomers

Studies of the atropisomeric enrichment of PCBs in environmental monitoring and laboratory studies require the use of several enantioselective columns. Unfortunately, the elution order of PCB atropisomers can change depending of the chiral

stationary phase (Kania-Korwel and Lehmler 2013). For example, the elution order of the PCB 84 atropisomers depends on the stationary phase of typical enantioselective gas and liquid chromatography columns (Tables 4 and 5). It is therefore important to establish the elution order of PCB atropisomers on these frequently used, commercially available columns. Moreover, a growing number of studies demonstrate that chiral PCBs are subject to atropselective biotransformation processes (Kania-Korwel and Lehmler 2016a, b; Lehmler et al. 2010) and display atropselective biological effects in fish and mammalian model systems (Chai et al. 2016a, b; Lehmler et al. 2005a; Pessah et al. 2009; Püttmann et al. 1990, 1989; Rodman et al. 1991; Xu et al. 2016; Yang et al. 2014). To fully understand the interactions of pure PCB atropisomers with cellular targets, such as the ryanodine receptor, it is important not only to unambiguously identify PCB atropisomers but also to establish their absolute structure.

Table 5 Elution order of PCB 84 atropisomers on different enantioselective gas chromatography columns

Columns ^a	Elution order		Reference
	Optical rotation (E_1/E_2)	Absolute structure (E_1/E_2)	
CP-Chirasil-Dex CB	(-)/(+)	(aR)/(aS)	Haglund (1996a), Kania-Korwel and Lehmler (2013), Konwick et al. (2006), this work
BGB-172	(-)/(+)	(aR)/(aS)	Kania-Korwel and Lehmler (2013), Konwick et al. (2006)
Cyclosil-B	(+)(-)	(aS)/(aR)	Kania-Korwel and Lehmler (2013)
HP-Chiral-20B	NR		Kania-Korwel and Lehmler (2013)
Chiral-Dex B-DM	NR		Kania-Korwel and Lehmler (2013)
Chiral-Dex B-PM	NR		Kania-Korwel and Lehmler (2013)

E_1 atropisomer eluting first on the column, E_2 atropisomer eluting second on the column, NR not resolved

^aThe Chirasil-Dex, Cyclosil-B, and HP-Chiral-20B columns were from Agilent (Santa Clara, CA, USA); the BGB-172 column was from BGB Analytics (Boecten, Switzerland); the Chiral-Dex B-DM and Chiral-Dex B-PM columns were from Supelco (St. Louis, MO, USA)

As discussed above, the PCB 84 atropisomer eluting first and second on the Nucleodex β -PM column corresponds to (aR)-(-)-PCB 84 and (aS)-(+)-PCB 84, respectively. In the case of methoxy, methylthionyl, and methylsulfonyl metabolites of chiral PCB 149, (aS)-atropisomers elute first on the Nucleodex β -PM column for substituents in the three positions of the PCB 149 moiety, whereas (aS)-atropisomers elute second for substituents in the four positions of the PCB 149 moiety (Pham-Tuan et al. 2005). Enantioselective gas chromatographic analysis with the β -cyclodextrin-based CP-Chirasil-Dex CB capillary column showed the same elution order as on the Nucleodex β -PM column, with (aR)-(-)-PCB 84 eluting first and (aS)-(+)-PCB 84 eluting second (Fig. 1). The same elution order of the PCB 84 atropisomers has been reported for the BGB-172 (20% *tert*-butyldimethylsilyl- β -cyclodextrin), but not the Cyclosil-B capillary column (30% heptakis (2,3-di-*O*-methyl-6-*O*-*t*-butyl dimethylsilyl)- β -cyclodextrin) (Table 5). The (aR)-atropisomer of PCB 132 and PCB 171 also eluted first on the BGB-172 capillary column, whereas (aR)-PCB 183 eluted second on this column.

Reinterpretation of chiral PCB 84 signatures and toxicity studies

The determination of the absolute structure of PCB 84 atropisomers for the first time allows the identification of the atropisomer that is enriched in environmental and other biological samples. Metabolism studies with recombinant CYP2B1 or rat liver microsomes indicate that (aR)-(-)-PCB 84 is more rapidly metabolized in rats (Kania-Korwel and Lehmler 2013; Warner et al. 2009). Consistent with the findings from these *in vitro* studies, (aS)-(+)-PCB 84 was slightly enriched in spleen of laboratory rats (EF = 0.52) (Kania-Korwel et al. 2006). Similarly, (aS)-(+)-PCB 84 was enriched in all tissues from mice (Lehmler et al. 2003). In contrast, (aR)-(-)-PCB 84 is enriched in both rainbow trout exposed to a mixture containing PCBs and pesticides (Konwick et al. 2006) and stranded cetaceans (Jimenez et al. 1999). Systematic studies of chiral signatures of PCBs in humans are limited (Kania-Korwel and Lehmler 2016b). Enantiomeric analysis of PCB 84 in breast milk showed no consistent enrichment of either the (aS)-(+)- or (aR)-(-)-atropisomer, with approximately half of the samples displaying near racemic chiral signatures (Bordajandi et al. 2008). (aS)-(+)-PCB 84 was significantly enriched in eggs of predatory birds from Donana National Park (Spain) with EF values ranging from 0.54 to 0.65 (Gomara and Gonzalez 2006).

Moreover, the absolute structure determinations reported in this study make it possible to unambiguously identify which PCB atropisomer has the more potent effects on, for example, biochemical measures linked to PCBs' developmental neurotoxicity. (aR)-(-)-PCB 84 and (aS)-(+)-PCB 84

atropselectively increase [3 H]-phorbol ester binding in rat cerebellar granule cells, with (aR)-(-)-PCB 84 being slightly more potent (Lehmler et al. 2005a). [3 H]Ryanodine binding analysis suggested that (aR)-(-)-PCB 84 is only slightly more potent than (aS)-(+)-PCB 84 toward sensitizing activation of ryanodine receptor 1 (RyR1) (Pessah et al. 2009).

Conclusions

In the present study, the absolute configurations of the atropisomers of PCB 84 were determined by X-ray diffraction. Based on this determination, (aR)-(-)-PCB 84 eluted first on the Nucleodex β -PM liquid chromatography and the CP-Chirasil-Dex CB capillary gas chromatography columns. Comparison of these elution orders to previously reported elution orders of PCB 84 and other chiral PCB congeners demonstrate that, similar to the optical rotation, the elution order of (aR)- vs. (aS)-atropisomers of PCBs on different enantioselective columns depends on the stationary phase. Knowledge of the absolute configuration of chiral PCBs, such as PCB 84, will advance both laboratory and environmental studies investigating the environmental transport and fate as well as the toxicity of these persistent organic pollutants.

Acknowledgements This work was supported by grants ES05605, ES013661, and ES017425 from the National Institute of Environmental Health Sciences/National Institutes of Health. The X8 Proteum diffractometer was funded by the National Science Foundation (MRI CHE0319176) and by the University of Kentucky (cost share). The content of this manuscript is solely the responsibility of the authors and does not necessarily represent the official views of the National Institute of Environmental Health Sciences/National Institutes of Health or the National Science Foundation.

References

- Bordajandi LR, Abad E, Gonzalez MJ (2008) Occurrence of PCBs, PCDD/Fs, PBDEs and DDTs in Spanish breast milk: enantiomeric fraction of chiral PCBs. *Chemosphere* 70:567–575
- Bruker-AXS (2006) APEX2. Bruker-AXS Inc., Madison
- Chai T, Cui F, Mu X, Yang Y, Wang C, Qiu J (2016a) Exploration of stereoselectivity in embryo-larvae (*Danio rerio*) induced by chiral PCB149 at the bioconcentration and gene expression levels. *PLoS One* 11
- Chai T, Cui F, Yin Z, Yang Y, Qiu J, Wang C (2016b) Chiral PCB 91 and 149 toxicity testing in embryo and larvae (*Danio rerio*): application of targeted metabolomics via UPLC-MS/MS. *Sci Rep*. doi:10.1038/srep33481 **Uk** 6
- Gomara B, Gonzalez MJ (2006) Enantiomeric fractions and congener specific determination of polychlorinated biphenyls in eggs of predatory birds from Donana National Park (Spain). *Chemosphere* 63: 662–669
- Grimm FA, Hu D, Kania-Korwel I, Lehmler HJ, Ludewig G, Hornbuckle KC, Duffel MW, Bergman A, Robertson LW (2015) Metabolism and metabolites of polychlorinated biphenyls. *Crit Rev Toxicol* 45: 245–272

- Haglund P (1996a) Enantioselective separation of polychlorinated biphenyl atropisomers using chiral high-performance liquid chromatography. *J Chromatogr A* 724:219–228
- Haglund P (1996b) Isolation and characterisation of polychlorinated biphenyl (PCB) atropisomers. *Chemosphere* 32:2133–2140
- Harju MT, Haglund P (1999) Determination of the rotational energy barriers of atropisomeric polychlorinated biphenyls. *Fresen J Anal Chem* 364:219–223
- Jimenez O, Jimenez B, Marsili L, Gonzalez MJ (1999) Enantiomeric ratios of chiral polychlorinated biphenyls in stranded cetaceans from the Mediterranean Sea. *Organohalogen Compd* 40:409–412
- Joshi SN, Vyas SM, Duffel MW, Parkin S, Lehmler HJ (2011) Synthesis of sterically hindered polychlorinated biphenyl derivatives. *Synthesis* 7:1045–1054
- Kania-Korwel I, Garrison AW, Avants JK, Hombuckle KC, Robertson LW, Sulkowski WW, Lehmler HJ (2006) Distribution of chiral PCBs in selected tissues in the laboratory rat. *Environ Sci Technol* 40:3704–3710
- Kania-Korwel I, Lehmler HJ (2013) Assigning atropisomer elution orders using atropisomerically enriched polychlorinated biphenyl fractions generated by microsomal metabolism. *J Chromatogr A* 1278:133–144
- Kania-Korwel I, Lehmler HJ (2016a) Chiral polychlorinated biphenyls: absorption, metabolism and excretion—a review. *Environ Sci Pollut Res* 23:2042–2057
- Kania-Korwel I, Lehmler HJ (2016b) Toxicokinetics of chiral polychlorinated biphenyls across different species—a review. *Environ Sci Pollut Res* 23:2058–2080
- Konwick BJ, Garrison AW, Black MC, Avants JK, Fisk AT (2006) Bioaccumulation, biotransformation, and metabolite formation of fipronil and chiral legacy pesticides in rainbow trout. *Environ Sci Technol* 40:2930–2936
- Krause L, Herbst-Irmer R, Sheldrick GM, Stalke D (2015) Comparison of silver and molybdenum microfocus X-ray sources for single-crystal structure determination. *J Appl Cryst* 48(1):3–10
- Lehmler HJ, Price DJ, Garrison AW, Birge WJ, Robertson LW (2003) Distribution of PCB 84 enantiomers in C57BL/6 mice. *Fresenius Environ Bull* 12:254–260
- Lehmler HJ, Robertson LW, Garrison AW, Kodavanti PRS (2005a) Effects of PCB 84 enantiomers on [³H]-phorbol ester binding in rat cerebellar granule cells and ⁴⁵Ca²⁺-uptake in rat cerebellum. *Toxicol Lett* 156:391–400
- Lehmler HJ, Robertson LW, Parkin S (2005b) 2,2',3,3',6-Pentachlorobiphenyl (PCB 84). *Acta Crystallogr Sect E: Struct Rep Online* 61:O3025–O3026
- Lehmler HJ, Harrad SJ, Huhnerfuss H, Kania-Korwel I, Lee CM, Lu Z, Wong CS (2010) Chiral polychlorinated biphenyl transport, metabolism, and distribution: a review. *Environ Sci Technol* 44:2757–2766
- Li X, Parkin S, Lehmler HJ (2014) 2,4-Di-chloro-1-iodo-6-nitro-benzene. *Acta Crystallogr E* 70:0607
- Mannschreck A, Pustet N, Robertson LW, Oesch F, Puttmann M (1985) Enantiomers of polychlorinated-biphenyls semipreparative enrichment by liquid-chromatography. *Liebigs Ann Chem*:2101–2103
- Parkin S, Moezzi B, Hope H (1995) XABS2: an empirical absorption correction program. *J Appl Cryst* 28(1):53–56
- Parsons S, Flack HD, Wagner T (2013) Use of intensity quotients and differences in absolute structure refinement. *Acta Crystallogr B* 69: 249–259
- Pessah IN, Lehmler HJ, Robertson LW, Perez CF, Cabrales E, Bose DD, Feng W (2009) Enantiomeric specificity of (–)-2,2',3,3',6,6'-hexachlorobiphenyl toward ryanodine receptor types 1 and 2. *Chem Res Toxicol* 22:201–207
- Pham-Tuan H, Larsson C, Hoffmann F, Bergman A, Froba M, Huhnerfuss H (2005) Enantioselective semipreparative HPLC separation of PCB metabolites and their absolute structure elucidation using electronic and vibrational circular dichroism. *Chirality* 17: 266–280
- Puttmann M, Oesch F, Robertson LW (1986) Characteristics of polychlorinated biphenyl (PCB) atropisomers. *Chemosphere* 15: 2061–2064
- Puttmann M, Mannschreck A, Oesch F, Robertson L (1989) Chiral effects in the induction of drug-metabolizing-enzymes using synthetic atropisomers of polychlorinated-biphenyls (PCBs). *Biochem Pharmacol* 38:1345–1352
- Puttmann M, Arand M, Oesch F, Mannschreck A, Robertson LW (1990) Chirality and the induction of xenobiotic-metabolizing enzymes: effects of the atropisomers of the polychlorinated biphenyl 2,2',3,4,4',6-hexachlorobiphenyl. In: Frank HHB, Testa B (eds) *Chirality and Biological Activity*. Alan R. Liss, Inc., New York, pp 177–184
- Reich S, Schurig V (1999) Enantiomerentrennung atropisomerer PCB mittels HPLC. *GIT Spezial* 1:15–16
- Rodman LE, Shedlofsky SI, Mannschreck A, Puttmann M, Swim AT, Robertson LW (1991) Differential potency of atropisomers of polychlorinated-biphenyls on cytochrome-P450 induction and uroporphyrin accumulation in the chick-embryo hepatocyte culture. *Biochem Pharmacol* 41:915–922
- Sheldrick GM (2008) A short history of SHELX. *Acta Cryst A* 64:112–122
- Sheldrick GM (2015) Crystal structure refinement with SHELXL. *Acta Crystallogr Sect C Struct Chem* 71:3–8
- Toda M, Matsumura C, Tsurukawa M, Okuno T, Nakano T, Inoue Y, Mori T (2012) Absolute configuration of atropisomeric polychlorinated biphenyl 183 enantiomerically enriched in human samples. *J Phys Chem A* 116:9340–9346
- Warner NA, Martin JW, Wong CS (2009) Chiral polychlorinated biphenyls are biotransformed enantioselectively by mammalian cytochrome p-450 isozymes to form hydroxylated metabolites. *Environ Sci Technol* 43:114–121
- Xu N, Mu P, Jia Q, Chai T, Yin Z, Yang S, Qiu J (2015) Comparison of enantioseparations of 19 chiral polychlorinated biphenyls by 5 different polysaccharides chiral columns. *Chin J Anal Chem* 43:795–801
- Xu N, Mu P, Yin Z, Jia Q, Yang S, Qian Y, Qiu J (2016) Analysis of the enantioselective effects of PCB 95 in zebrafish (*Danio rerio*) embryos through targeted metabolomics by UPLC-MS/MS. *Plos One* 11:e0160584
- Yang DR, Kania-Korwel I, Ghogha A, Chen H, Stamou M, Bose DD, Pessah IN, Lehmler HJ, Lein PJ (2014) PCB 136 atropselectively alters morphometric and functional parameters of neuronal connectivity in cultured rat hippocampal neurons via ryanodine receptor-dependent mechanisms. *Toxicol Sci* 138:379–392
- Yin W, Wu C, Fnag L, Zhang A (2012) Enantiomer separation of polychlorinated biphenyls on chiral chromatographic columns of cellulose and amylose by high-performance liquid chromatography. *J Zhengjiang Univ Technol* 40:35–38